NURETH14-633

KOREAN DEVELOPMENT OF ADVANCED THERMAL-HYDRAULIC CODES FOR WATER REACTORS AND HTGRS: SPACE AND GAMMA

Hee Cheon NO^{1,2}

¹ 1 Department of Nuclear and Quantum Engineering, Korea Advanced Institute of Science and Technology 373-1 Guseong-dong Yuseong-gu, Daejeon, 305-701, Korea Tel: 82-42-350-3829, Fax: 82-42-350-3810,

Email: hcno@kaist.ac.kr

2 Department of Nuclear Engineering, Khalifa Üniversity of Science, Technology & Research (KUSTAR) P.O.Box 127788, Abu Dhabi, UAE

Abstract

Korea has been developing SPACE(Safety and Performance Analysis CodE) and GAMMA(GAs Multicomponent Mixture Analysis) codes for safety analysis of PWRs and HTGRs, respectively. SPACE is being developed by the Korea nuclear industry, which is a thermal-hydraulic analysis code for safety analysis of a PWR. It will replace outdated vendor supplied codes and will be used for the safety analysis of operating PWR and the design of an advanced PWR. It consists of the up-to-date physical models of two-phase flow dealing with multi-dimensional two-fluid, three-field flow. The GAMMA code consists of the multi-dimensional governing equations consisting of the basic equations for continuity, momentum conservation, energy conservation of the gas mixture, and mass conservation of n species. GAMMA is based on a porous media model so that we can deal with the thermo-fluid and chemical reaction behaviors in a multicomponent mixture system as well as heat transfer within the solid components, free and forced convection between a solid and a fluid, and radiative heat transfer between the solid surfaces. GAMMA has a model for helium turbines for HTGRs based on the throughflow calculation. We performed extensive code assessment for the V&V of SPACE and GAMMA.

1. Introduction

Amazingly the Korean first nuclear power construction program initiated when Korean annual income per person was about \$200. Just before the TMI accident took place in 1979, the Korean first nuclear power plant, Kori-1 was commercially started to operate in 1978 on turn-key contract basis. Just after the Chernobyl accident happened in 1986 the Korean nuclear industry boldly initiated and completed the technology self-reliance program of nuclear power plants to develop OPR1000 in 1995 when the Western countries abandoned their own nuclear program. As soon as we completed OPR-100 in 1995, Korea initiated and completed the development program of APR-1400 in 2001. Even after Korean IMF crisis happened in 1997, we did not stop the development program of APR-1400 even though several national programs stopped. In early 2010, Korea exported 4 APR-1400 reactors to the United Arab Emirates.

Even though we can export our nuclear power plants, we still depend on safety analysis tools offered by foreign vendor supply for the safety analysis of nuclear power plants, most of which were developed in 1970s. Actually, we planned the development of the safety tools for the safety analysis of PWRs in 1996. Unfortunately, the program stopped because of the Korean IMF crisis. After the recovery of the crisis KAIST and KAERI launched the development of the multi-dimensional thermal-hydraulic system tool, GAMMA for the safety analysis of HTGRs in 2002. Late, INL joined the development program through INERI. GAMMA has been advanced to implement extensive chemical reaction models, 2-D turbomachinary models, and multi-dimensional transient neutronics models. Finally, in 2006 the Korean nuclear industry launched the SPACE code development project to develop a new thermal-hydraulics system analysis code: In the SPACE code we are implementing the advanced physical models of two-phase flow: multi-dimensional and multi-field physical models. Also, the programming language for the GAMMA and SPACE codes is C++ for new generation of engineers who are more comfortable with C/C++ than FORTRAN language.

This paper describes overall features of SPACE code including hydraulic models and physical models and shows the code assessment results for several conceptual and separate effect test problems.

2. Models of SPACE Code

2.1 Subheading in a heading section

The main feature of SPACE is to solve the two-fluid, three field governing equations described in Ref. 1. The mass conservation equations of vapor, continuous liquid, droplet phase, and non-condensable gas are as follows:

Continuity equation for vapor phase:

$$\varepsilon \frac{\partial}{\partial t} (\alpha_g \rho_v) + \nabla \cdot (\varepsilon \alpha_g \rho_v \mathbf{U}_g) = \varepsilon (\Gamma_l + \Gamma_d)$$
 (1)

Continuity equation for continuous liquid phase:

$$\varepsilon \frac{\partial}{\partial t} (\alpha_l \rho_l) + \nabla \cdot (\varepsilon \alpha_l \rho_l \mathbf{U}_l) = \varepsilon (-\Gamma_l - S_E + S_D)$$
 (2)

Continuity equation for droplet phase:

$$\varepsilon \frac{\partial}{\partial t} (\alpha_d \rho_d) + \nabla \cdot (\varepsilon \alpha_d \rho_d \mathbf{U}_d) = \varepsilon (-\Gamma_d + S_E - S_D)$$
 (3)

Continuity equation for non-condensable gas:

$$\varepsilon \frac{\partial}{\partial t} (\alpha_g \rho_n) + \nabla \cdot (\varepsilon \alpha_g \rho_n \mathbf{U}_g) = 0 \tag{4}$$

In the above conservation equations, the subscripts v, ℓ , d, g, and n refer to the vapor, continuous liquid, droplet, vapor/non-condensable gas mixture and non-condensable gas mixture, respectively. Here, Γ_l , Γ_d represent the mass transfers at continuous liquid-vapor and droplet-vapor interfaces. Also, S_E , S_D denote entrainment and de-entrainment in the two liquid fields, respectively.

The momentum conservation equations of gas, continuous liquid, and droplet phase are expressed as follows.

Momentum equation for vapor phase:

$$\varepsilon \frac{\partial \mathbf{U}_{g}}{\partial t} + \nabla \cdot \left(\varepsilon \mathbf{U}_{g} \mathbf{U}_{g}\right) - \mathbf{U}_{g} \nabla \cdot \left(\varepsilon \mathbf{U}_{g}\right) \\
= -\frac{\varepsilon}{\rho_{g}} \nabla P - \frac{\varepsilon F_{wg}}{\alpha_{g} \rho_{g}} \mathbf{U}_{g} - \frac{\varepsilon F_{gd}}{\alpha_{g} \rho_{g}} (\mathbf{U}_{g} - \mathbf{U}_{d}) - \frac{\varepsilon F_{gl}}{\alpha_{g} \rho_{g}} (\mathbf{U}_{g} - \mathbf{U}_{l}) + \varepsilon \mathbf{B} \\
+ \frac{\varepsilon}{\alpha_{g} \rho_{g}} \left(\Gamma_{l,E} \mathbf{U}_{l} + \Gamma_{d,E} \mathbf{U}_{d} - \Gamma_{l,E} \mathbf{U}_{g} - \Gamma_{d,E} \mathbf{U}_{g}\right) \\
- \varepsilon C_{g,gd} \alpha_{d} \frac{\rho_{m,gd}}{\rho_{g}} \frac{\partial (\mathbf{U}_{g} - \mathbf{U}_{d})}{\partial t} - \varepsilon C_{g,gl} \alpha_{l} \frac{\rho_{m,gl}}{\rho_{g}} \frac{\partial (\mathbf{U}_{g} - \mathbf{U}_{l})}{\partial t}$$
(5)

Momentum equation for continuous liquid phase:

$$\varepsilon \frac{\partial \mathbf{U}_{l}}{\partial t} + \nabla \cdot (\varepsilon \mathbf{U}_{l} \mathbf{U}_{l}) - \mathbf{U}_{l} \nabla \cdot (\varepsilon \mathbf{U}_{l})$$

$$= -\frac{\varepsilon}{\rho_{l}} \nabla P - \frac{\varepsilon F_{wl}}{\alpha_{l} \rho_{l}} \mathbf{U}_{l} - \frac{\varepsilon F_{lg}}{\alpha_{l} \rho_{l}} (\mathbf{U}_{l} - \mathbf{U}_{g}) + \varepsilon \mathbf{B}$$

$$+ \frac{\varepsilon}{\alpha_{l} \rho_{l}} \left(-\Gamma_{l,C} \mathbf{U}_{l} + \Gamma_{l,C} \mathbf{U}_{g} + S_{D} \mathbf{U}_{d} - \mathbf{U}_{l} S_{D} \right) - \varepsilon C_{g,gl} \alpha_{g} \frac{\rho_{m,gl}}{\rho_{l}} \frac{\partial (\mathbf{U}_{l} - \mathbf{U}_{g})}{\partial t}$$
(6)

where

$$\Gamma_I = \Gamma_{IF} - \Gamma_{IC}$$

Momentum equation for droplet phase:

$$\varepsilon \frac{\partial \mathbf{U}_{d}}{\partial t} + \nabla \cdot (\varepsilon \mathbf{U}_{d} \mathbf{U}_{d}) - \mathbf{U}_{d} \nabla \cdot (\varepsilon \mathbf{U}_{d})$$

$$= -\frac{\varepsilon}{\rho_{d}} \nabla P - \frac{\varepsilon F_{wd}}{\alpha_{d} \rho_{d}} \mathbf{U}_{d} - \frac{\varepsilon F_{dg}}{\alpha_{d} \rho_{d}} (\mathbf{U}_{d} - \mathbf{U}_{g}) + \varepsilon \mathbf{B}$$

$$+ \frac{\varepsilon}{\alpha_{d} \rho_{d}} \left(-\Gamma_{d,C} \mathbf{U}_{d} + \Gamma_{d,C} \mathbf{U}_{g} + S_{E} \mathbf{U}_{l} - S_{E} \mathbf{U}_{d} \right) - \varepsilon C_{g,dg} \alpha_{g} \frac{\rho_{m,dg}}{\rho_{d}} \frac{\partial (\mathbf{U}_{d} - \mathbf{U}_{g})}{\partial t}$$
(7)

where $\Gamma_d = \Gamma_{d,E} - \Gamma_{d,C}$

The energy conservation equations for the vapor/gas mixture, continuous liquid, droplet phases can be expressed at thermal non-equilibrium states of three fields as follows:

$$\frac{\partial (\varepsilon \alpha_{g} (\rho_{v} e_{v} + \rho_{n} e_{n}))}{\partial t} + \nabla \cdot \left(\varepsilon \alpha_{v} (\rho_{v} e_{v} + \rho_{n} e_{n}) \mathbf{U}_{g} \right)
= -\varepsilon P \frac{\partial \alpha_{g}}{\partial t} - P \nabla \cdot \left(\varepsilon \alpha_{g} \mathbf{U}_{g} \right) + \varepsilon \left(Q_{iv-l} + \Gamma_{l} h_{vl}^{*} + \Gamma_{d} h_{vd}^{*} + Q_{iv-d} + Q_{l-n} + Q_{d-n} \right)$$
(8)

$$\frac{\partial (\varepsilon \alpha_{l} \rho_{l} e_{l})}{\partial t} + \nabla \cdot \left(\varepsilon \alpha_{l} \rho_{l} e_{l} \mathbf{U}_{l}\right) = -\varepsilon P \frac{\partial \alpha_{l}}{\partial t} - P \nabla \cdot \left(\varepsilon \alpha_{l} \mathbf{U}_{l}\right) + \varepsilon \left(Q_{il} - \Gamma_{l} h_{l}^{*} - S_{E} h_{l} + S_{D} h_{d} - Q_{l-n}\right)$$

$$\tag{9}$$

$$\frac{\partial (\varepsilon \alpha_d \rho_d e_d)}{\partial t} + \nabla \cdot \left(\varepsilon \alpha_d \rho_d e_d \mathbf{U}_d\right) = -\varepsilon P \frac{\partial \alpha_d}{\partial t} - P \nabla \cdot \left(\varepsilon \alpha_d \mathbf{U}_d\right) + \varepsilon \left(\underline{Q}_{id} - \Gamma_d h_d^* + S_E h_l - S_D h_d - \underline{Q}_{d-n}\right)$$
(10)

where Q represents the interfacial heat transfer rate per volume.

Through the staggered mesh layout spatially and semi-implicit scheme temporally maintaining the conservative and transportive properties, the governing equations are discretized as follows.

$$\varepsilon V_{p} \frac{\alpha_{g}^{n} \rho_{n}^{n} - \alpha_{g} \rho_{n}}{\Delta t} + \sum_{E \in \mathcal{D}} \varepsilon^{E} \alpha_{g}^{E} \rho_{n}^{E} \left(\iota_{p}^{E} U_{gn}^{n} A^{E} \right) = 0$$

$$(11)$$

Vapor mass conservation equation:

$$\varepsilon V_{P} \frac{\alpha_{g}^{n} \rho_{v}^{n} - \alpha_{g} \rho_{v}}{\Delta t} + \sum_{k \in D} \varepsilon^{E d} \alpha_{g}^{E d} \rho_{v}^{E} \left(\iota_{P}^{E} U_{gn}^{n} A^{E} \right) = \varepsilon V_{P} \left(\Gamma_{l} + \Gamma_{d} \right)^{n}$$

$$(12)$$

Droplet mass conservation equation:

$$\varepsilon V_{P} \frac{\alpha_{d}^{n} \rho_{d}^{n} - \alpha_{d} \rho_{d}}{\Delta t} + \sum_{E \in D} \varepsilon^{E d} \alpha_{d}^{E d} \rho_{d}^{E} \left(\iota_{P}^{E} U_{dn}^{n} A^{E} \right) = \varepsilon V_{P} \left(-\Gamma_{d}^{n} + S_{E} - S_{D} \right)$$

$$\tag{13}$$

Continuous liquid mass conservation equation:

$$\varepsilon V_{p} \frac{\alpha_{l}^{n} \rho_{l}^{n} - \alpha_{l} \rho_{l}}{\Delta t} + \sum_{E \in P} \varepsilon^{E \ d} \alpha_{l}^{E \ d} \rho_{l}^{E} \left(\iota_{p}^{E} U_{ln}^{n} A^{E} \right) = \varepsilon V_{p} \left(-\Gamma_{l}^{n} - S_{E} + S_{D} \right)$$

$$(14)$$

Gas energy conservation equation:

$$\varepsilon V_{p} \frac{\alpha_{g}^{n} \left(\rho_{v}^{n} e_{v}^{n} + \rho_{n}^{n} e_{n}^{n}\right) - \alpha_{g} \left(\rho_{v} e_{v} + \rho_{n} e_{n}\right)}{\Delta t}$$

$$+ \sum_{E \in P} \iota_{p}^{E} \varepsilon^{E} \alpha_{g}^{E} \left(^{d} \rho_{v}^{E} e_{v}^{E} + ^{d} \rho_{n}^{E} e_{n}^{E}\right) \left(U_{gn}^{n} A^{E}\right) + P \sum_{E \in P} \iota_{p}^{E} \varepsilon^{E} \alpha_{g}^{E} U_{gn}^{n} A^{E}$$

$$= \varepsilon V_{p} \left[-P \frac{\alpha_{g}^{n} - \alpha_{g}}{\Delta t} + Q_{iv-l}^{n} + \Gamma_{l}^{n} h_{vl}^{*} + \Gamma_{d}^{n} h_{vd}^{*} + Q_{iv-d}^{n} + Q_{l-n}^{n} + Q_{d-n}^{n} + Q_{wg}^{n} \right]$$

$$(4/18)$$

Droplet energy conservation equation:

$$\varepsilon V_{P} \frac{\alpha_{d}^{n} \rho_{d}^{n} e_{d}^{n} - \alpha_{d} \rho_{d} e_{d}}{\Delta t} + \sum_{E \in P} t_{P}^{E} \varepsilon^{E} \alpha_{d}^{E} \alpha_{d}^{E} \rho_{d}^{E} e_{d}^{E} \left(U_{dn}^{n} A^{E} \right) + P \sum_{E \in P} t_{P}^{E} \varepsilon^{E} \alpha_{d}^{E} U_{dn}^{n} A^{E}$$

$$= \varepsilon V_{P} \left[-P \frac{\alpha_{d}^{n} - \alpha_{d}}{\Delta t} + Q_{id}^{n} - \Gamma_{d}^{n} h_{d}^{*} + S_{E} h_{l} - S_{D} h_{d} - Q_{d-n}^{n} + Q_{wd} \right]$$

$$(16)$$

Continuous liquid energy conservation equation:

$$\varepsilon V_{P} \frac{\alpha_{l}^{n} \rho_{l}^{n} e_{l}^{n} - \alpha_{l} \rho_{l} e_{l}}{\Delta t} + \sum_{E \in P} \iota_{P}^{E} \varepsilon^{E} \alpha_{l}^{E} \rho_{l}^{E} e_{l}^{E} \left(U_{ln}^{n} A^{E} \right) + P \sum_{E \in P} \iota_{P}^{E} \varepsilon^{E} \alpha_{l}^{E} U_{ln}^{n} A^{E}$$

$$= \varepsilon V_{P} \left[-P \frac{\alpha_{l}^{n} - \alpha_{l}}{\Delta t} + Q_{il}^{n} - \Gamma_{l}^{n} h_{l}^{*} - S_{E} h_{l} + S_{D} h_{d} - Q_{l-n}^{n} + Q_{wl} \right]$$

$$(17)$$

Gas momentum conservation equation:

$$\varepsilon^{E}V^{E}\frac{\left(U_{gn}^{E}\right)^{n}-U_{gn}^{E}}{\Delta t}+\varepsilon_{(k)}^{Neighbor}{}^{d}U_{g(k)}^{Neighbor}\left(A_{(k)}^{Neighbor}U_{g(k)}^{Neighbor}\right)-\varepsilon_{(k)}^{Ownerd}U_{g(k)}^{Owner}\left(A_{(k)}^{Owner}U_{g(k)}^{Owner}\right)$$

$$+\sum_{E\subseteq Owner, typ\neq k}\varepsilon^{E'}{}^{d}XU_{g(k)}^{Fhcell}(\iota_{Owner}^{E'}\frac{1}{2}U_{gn}^{E'}A^{E'})+\sum_{E\subseteq Neighbor, typ\neq k}\varepsilon^{E'}{}^{d}XU_{g(k)}^{ghcell}(\iota_{Neighbor}^{E'}\frac{1}{2}U_{gn}^{E'}A^{E'})$$

$$+F_{g(k)}V^{E}-U_{gn}^{E}\varepsilon_{(k)}^{Neighbor}\left(A_{(k)}^{Neighbor}U_{g(k)}^{Neighbor}\right)+U_{gn}^{E}\varepsilon_{(k)}^{Owner}\left(A_{(k)}^{Owner}U_{g(k)}^{Owner}\right)$$

$$-U_{gn}^{E}\sum_{E\subseteq Owner, typ\neq k}\varepsilon^{E'}(\iota_{Owner}^{E'}\frac{1}{2}U_{gn}^{E'}A^{E'})-U_{gn}^{E}\sum_{E'\subseteq Neighbor, typ\neq k}\varepsilon^{E'}(\iota_{Neighbor}^{E'}\frac{1}{2}U_{gn}^{E'}A^{E'})$$

$$= \frac{1}{\rho_{g}} \varepsilon^{E} A^{E} \left(P_{Owner}^{n} - P_{Neighbor}^{n}\right)$$

$$+ \frac{\varepsilon^{E} V^{E}}{\alpha_{g} \rho_{g}} \begin{bmatrix} -F_{wg} \left(U_{gn}^{E}\right)^{n} - F_{gd} \left(U_{gn}^{E} - U_{dn}^{E}\right)^{n} - F_{gl} \left(U_{gn}^{E} - U_{ln}^{E}\right)^{n} + \alpha_{g} \rho_{g} \mathbf{B} \cdot \mathbf{n}^{E} \\ + \Gamma_{l,E} \left(U_{ln}^{E}\right)^{n} + \Gamma_{d,E} \left(U_{dn}^{E}\right)^{n} - \Gamma_{l,E} \left(U_{gn}^{E}\right)^{n} - \Gamma_{d,E} \left(U_{gn}^{E}\right)^{n} \\ -C_{g,gd} \alpha_{g} \alpha_{d} \rho_{m,gd} \frac{\left(U_{gn}^{E} - U_{dn}^{E}\right)^{n} - \left(U_{gn}^{E} - U_{dn}^{E}\right)}{\Delta t} \\ -C_{g,gl} \alpha_{g} \alpha_{l} \rho_{m,gl} \frac{\left(U_{gn}^{E} - U_{ln}^{E}\right)^{n} - \left(U_{gn}^{E} - U_{ln}^{E}\right)}{\Delta t} \end{bmatrix}$$

Droplet momentum conservation equation:

$$\varepsilon^{E}V^{E} \frac{\left(U_{dn}^{E}\right)^{n} - U_{dn}^{E}}{\Delta t} + \varepsilon_{(k)}^{Neighbor} {}^{d}U_{d(k)}^{Neighbor} \left(A_{(k)}^{Neighbor}U_{d(k)}^{Neighbor}\right) - \varepsilon_{(k)}^{Ownerd}U_{d(k)}^{Owner} \left(A_{(k)}^{Owner}U_{d(k)}^{Owner}\right) \\
+ \sum_{E \subseteq Owner, typ \neq k} \varepsilon^{E^{+}} {}^{d}X U_{d(k)}^{Fhcell} \left(t_{Owner}^{E^{+}} \frac{1}{2} U_{dn}^{E^{+}} A^{E^{+}}\right) + \sum_{E \subseteq Neighbor, typ \neq k} \varepsilon^{E^{+}} {}^{d}X U_{d(k)}^{Bhcell} \left(t_{Neighbor}^{E^{+}} \frac{1}{2} U_{dn}^{E^{+}} A^{E^{+}}\right) \\
+ F_{d(k)}V^{E} - U_{dn}^{E} \varepsilon_{(k)}^{Neighbor} \left(A_{(k)}^{Neighbor}U_{d(k)}^{Neighbor}\right) + U_{dn}^{E} \varepsilon_{(k)}^{Owner} \left(A_{(k)}^{Owner}U_{d(k)}^{Owner}\right) \\
- U_{dn}^{E} \sum_{E \subseteq Owner, typ \neq k} \varepsilon^{E^{+}} \left(t_{Owner}^{E^{+}} \frac{1}{2} U_{dn}^{E^{+}} A^{E^{+}}\right) - U_{dn}^{E^{+}} \sum_{E \subseteq Neighbor, typ \neq k} \varepsilon^{E^{+}} \left(t_{Neighbor}^{E^{+}} \frac{1}{2} U_{dn}^{E^{+}} A^{E^{+}}\right) \\
= \frac{1}{\rho_{d}} \varepsilon^{E} A^{E} \left(P_{Owner}^{n} - P_{Neighbor}^{n}\right) \\
+ \frac{\varepsilon^{E} V^{E}}{\alpha_{d} \rho_{d}} \begin{bmatrix} -F_{wd} \left(U_{dn}^{E}\right)^{n} - F_{dg} \left(U_{dn}^{E} - U_{gn}^{E}\right)^{n} + \alpha_{d} \rho_{d} \mathbf{B} \cdot \mathbf{n}^{E} \\
-\Gamma_{d,C} \left(U_{dn}^{E}\right)^{n} + \Gamma_{d,C} \left(U_{gn}^{E}\right)^{n} + S_{E} \left(U_{in}^{E}\right)^{n} - S_{E} \left(U_{dn}^{E}\right)^{n} \\
-C_{g,dg} \alpha_{d} \alpha_{g} \rho_{m,dg} \frac{\left(U_{dn}^{E} - U_{gn}^{E}\right)^{n} - \left(U_{dn}^{E} - U_{gn}^{E}\right)}{\Delta t} \end{bmatrix} \right]$$
(19)

Continuous liquid momentum conservation equation:

$$\varepsilon^{E}V^{E} \frac{\left(U_{ln}^{E}\right)^{n} - U_{ln}^{E}}{\Delta t} + \varepsilon_{(k)}^{Neighbor} {}^{d}U_{l(k)}^{Neighbor}\left(A_{(k)}^{Neighbor}U_{l(k)}^{Neighbor}\right) - \varepsilon_{(k)}^{Ownerd}U_{l(k)}^{Owner}\left(A_{(k)}^{Owner}U_{l(k)}^{Owner}\right) \\
+ \sum_{E \subseteq Owner, typ \neq k} \varepsilon^{E^{+}} X U_{l(k)}^{Fhcell}\left(\iota_{Owner}^{E^{+}} \frac{1}{2} U_{ln}^{E^{+}} A^{E^{+}}\right) + \sum_{E \subseteq Neighbor, typ \neq k} \varepsilon^{E^{+}} X U_{l(k)}^{Bhcell}\left(\iota_{Neighbor}^{E^{-}} \frac{1}{2} U_{ln}^{E^{+}} A^{E^{+}}\right) \\
+ F_{l(k)}V^{E} - U_{ln}^{E} \varepsilon_{(k)}^{Neighbor}\left(A_{(k)}^{Neighbor}U_{l(k)}^{Neighbor}\right) + U_{ln}^{E} \varepsilon_{(k)}^{Owner}\left(A_{(k)}^{Owner}U_{l(k)}^{Owner}\right) \\
- U_{ln}^{E} \sum_{E \subseteq Owner, typ \neq k} \varepsilon^{E^{+}}\left(\iota_{Owner}^{E^{-}} \frac{1}{2} U_{ln}^{E^{+}} A^{E^{+}}\right) - U_{ln}^{E^{-}} \sum_{E \subseteq Neighbor, typ \neq k} \varepsilon^{E^{+}}\left(\iota_{Neighbor}^{E^{-}} \frac{1}{2} U_{ln}^{E^{+}} A^{E^{+}}\right) \\
= \frac{1}{\rho_{l}} \varepsilon^{E} A^{E}\left(P_{Owner}^{n} - P_{Neighbor}^{n}\right) \\
+ \frac{\varepsilon^{E}V^{E}}{\alpha_{l}\rho_{l}} \begin{bmatrix} -F_{wl}\left(U_{ln}^{E}\right)^{n} - F_{lg}\left(U_{ln}^{E^{-}} - U_{gn}^{E^{-}}\right)^{n} + \alpha_{l}\rho_{l}\mathbf{B} \cdot \mathbf{n}^{E^{-}} \\
-\Gamma_{l,C}\left(U_{ln}^{E^{-}}\right)^{n} + \Gamma_{l,C}\left(U_{gn}^{E^{-}}\right)^{n} + S_{D}\left(U_{ln}^{E^{-}} - U_{gn}^{E^{-}}\right) \\
-C_{g,lg}\alpha_{l}\alpha_{g}\rho_{m,lg} \frac{\left(U_{ln}^{E^{-}} - U_{gn}^{E^{-}}\right)^{n} - \left(U_{ln}^{E^{-}} - U_{gn}^{E^{-}}\right)}{\Delta t}$$
(20)

The additional force terms, $F_{\phi(k)}$, represent the centrifugal and Coriolis force expressed as

Cartesian coordinate($x, y, z: U_x, U_y, U_z$):

$$F_{\phi(1)} = 0, \quad F_{\phi(2)} = 0, \quad F_{\phi(3)} = 0$$
 (21)

Cylindrical coordinate $(r, \theta, z: U_r, U_\theta, U_z)$:

$$F_{\phi(1)} = -\frac{U_{\phi(2)}^2}{r}, \quad F_{\phi(2)} = \frac{U_{\phi(1)}U_{\phi(2)}}{r}, \quad F_{\phi(3)} = 0$$

In order to solve the above non-linear algebraic equations we adopt the Newton-Raphson method. As the primary variables used in SPACE we select partial pressure of the non-condensable gas mixture (P_n) , phasic temperatures (T_g, T_i, T_d) , phasic volume fractions (α_v, α_d) , total pressure (P), and phasic velocities (U_g, U_l, U_d) . Then, we can generate the system pressure matrix containing the N x N system of pressure equations. The matrix is solved simultaneously at each time step, using the sparse matrix solver.

2.2 Models and Correlations

In order to develop the physical models and correlations for the SPACE code, we extensively reviewed the physical models used in major safety analysis codes: RELAP5 [2], TRAC-M [3], COBRA-TF [4], CATHARE [5] and MARS [6]. Additionally, we did an extensive literature survey for the incorporation of the up-to-date physical models into the SPACE code. The physical models and correlations of the SPACE code are categorized into five packages; i) a flow regime selection package, ii) a wall and interfacial friction package, iii) an interfacial heat and mass transfer package, iv) a droplet entrainment and de-entrainment package and v) a wall heat transfer package. Detail descriptions of models and correlation packages for the SPACE code are described in Ref. [7].

The SPACE code has two basic flow regime maps: horizontal and vertical flow regime maps. The vertical and horizontal flow regime maps depend on inclined sine angle in the cell with interpolation between them: $0 < |\sin \phi| \le 1/3$ and $2/3 \le |\sin \phi| \le 1$. Each flow regime map consists of bubbly, slug/cap-bubble, interpolation, annular-mist, stratified, and transition flow regimes. A hot wall flow regime map is used for post-dryout regime.

Two kinds of physical models for interfacial area concentration are required for vapor-continuous liquid interface and vapor-dispersed liquid interface. Interfacial area concentration for a slug flow is sum of interfacial area concentrations for small and Taylor bubbles. The interfacial area concentration in annular-mist flow consist of liquid film flowing and droplets carried by vapor. In the same way as the interfacial area concentration, the interfacial heat transfer coefficients for slug flow is sum of the interfacial heat transfer coefficients for small and Taylor bubbles.

The drift flux model is used to obtain an interfacial friction factor as a default model for bubbly and slug flow conditions in a vertical channel.

For the wall friction factor in two-phase flow the Churchill correlation [8] developed for single phase flow is used with the introduction of a two-phase multiplier obtained from modified Baroczy correlation [9]. We adopt a method proposed by Chisholm [10] for the partition of the total two-phase friction pressure drop into the wall friction pressure drops for continuous liquid, gas and dispersed liquid fields. We use the Churchill correlation for horizontally stratified flow.

Physical models for droplet entrainment and de-entrainment from a continuous liquid and to a continuous liquid have been investigated through extensive literature survey and experimental assessment of their candidates using SPACE. For vertical annular-mist flow we propose to use

Okawa-Kataoka models [11] for entrainment and deentrainment while we do to use Pan-Hanratty [12] model and Paras-Karabelas [13] for entrainment and deentrainment for horizontal annularmist flow.

Physical models for wall-to-fluid heat transfer are classified into 12 physical modes: liquid phase natural convection, liquid phase forced convection, subcooled and saturated nucleate boiling, critical heat flux, transition boiling, film boiling, vapor phase convection and condensation heat transfer. Figure 1 shows the flow chart for the selection of the heat transfer modes described in Ref. 1. One of the unique features of a wall-to-fluid heat transfer package of the SPACE code is to adopt a look-up table method for a film boiling region instead of a conventional correlation method. Use of the minimum film boiling temperature is suggested for the boundary between transition and film boiling heat transfer modes. We incorporate the reflood heat transfer package as a separate one into the heat structure model in order to consider the two-dimensional conduction effect. We propose the model for heat flux partition into continuous liquid, dispersed liquid and vapor fields for the source terms of the field equations.

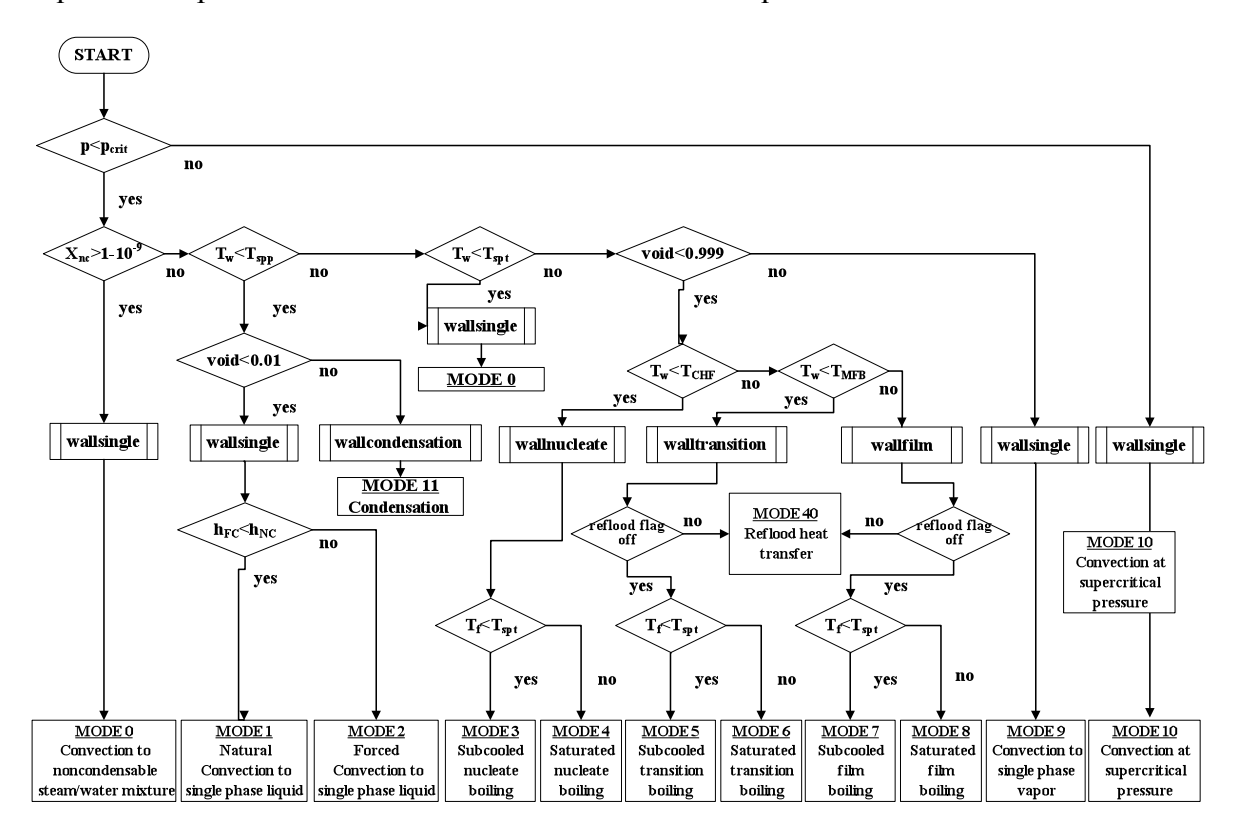


Figure 1. Heat transfer mode transition map

2.3 Models for Special Processes, Components, and Heat Structure

SPACE has special process models for choking of discharged or internal flow, limitation of countercurrent flow, off-take, water level tracking, and the abrupt change of the flow area.

Three two-phase choking models implemented: Ransom and Trapp [14], Moody [15], and Henry-Fauske [16]. Wallis [17], Kutateladze [18], and Bankoff [19] correlations are integrated for the model of limitation of countercurrent flow. Four offtake models are implemented depending on water levels and opening locations: top offtake and bottom offtake models, and two side offtake models. The level tracking model is applied to a vertical cell or a series of vertical cells.

System component models are implemented into SPACE: models for centrifugal pump, valves, pressurizer, safety injection tank, mixing of emergency core cooling water and the steam, separator, and turbine.

1-D and 2-D heat conduction models are implemented in SPACE. Two-dimensional model is implemented to calculate two-dimensional temperature distribution of a fuel rod, in axial and radial directions, especially in case of reflood.

3. Code Assessment

As shown in Table 1, SPACE code assessment using 9 test facilities and CFD calculation results has been performed.

	Test Facility	Purposes
1	Nine-volume water overs steam	to check the gravitational head effect and the development of countercurrent flow from an initial sharp liquid-vapor interface
2	Nitrogen-water manometer problem	to check the non-condensable gas state calculation and the momentum formulation for periodic flow
3	Branch reentrant tee problem	
4	Cross-flow tee problem	
5	Cross tank problem	to test flow anomalies that may appear as recirculating two-phase or single-phase flows using the cross-flow junction feature in the code to model multidimensional effects
6	Horizontally Stratified Countercurrent Flow	to verify that the speed of propagation for a void wave is compared with theoretical value
7	Multi-Dimensional Problems	to check the multi-dimensional flow models including multi- dimensional formulation of the momentum equations

8	GE level swell	To check the correct predictions of level swell phenomena, accurate flashing and interface drag models
9	Bennett's heated	To check the correct predictions of the wall temperature, CHF location, and droplet entrainment under LOCA condition
	tube experiments	,

Table 1. Assessment matrix for SPACE V&V

4. Description of GAMMA Code

4.1 Governing equations

The GAMMA(GAs Multicomponent Mixture Analysis) code consists of the multi-dimensional governing equations consisting of the basic equations for continuity, momentum conservation, energy conservation of the gas mixture, and mass conservation of n species (He, N2, O2, CO, CO2, H2O, other noncondensables) [20,21,22]. The derivation of the governing equations of GAMMA is based on a porous media model so that we can deal with the thermo-fluid and chemical reaction behaviors in a multicomponent mixture system as well as heat transfer within the solid components, free and forced convection between a solid and a fluid, and radiative heat transfer between the solid surfaces.

The equation of continuity for the gas mixture:

$$\varphi \frac{\partial \rho}{\partial t} + \nabla \cdot (\rho \mathbf{u}) = \varphi \sum_{s} R_{s}$$
 (21)

The equation of momentum conservation:

$$\rho \left(\frac{1}{\varphi} \frac{\partial \mathbf{u}}{\partial t} + \frac{1}{\varphi^2} \mathbf{u} \cdot \nabla \mathbf{u} \right) = -\nabla P + \frac{1}{\varphi} \nabla \cdot \left(\mu \nabla \mathbf{u} \right) - \frac{\mu}{K} \mathbf{u} - \frac{C_F \rho}{\sqrt{K}} |\mathbf{u}| \mathbf{u} + \rho \mathbf{g}$$
 (22)

The equation of sensible energy conservation:

$$\varphi \frac{\partial}{\partial t} (\rho H) + \nabla \cdot (\rho \mathbf{u} H) = \nabla \cdot \left[\left(\varphi \lambda_f + \lambda_{disp} \right) \nabla T_f \right] - \nabla \cdot \left(\varphi \sum_{s=1}^m H_s \mathbf{J}_s \right)$$

$$- \varphi \sum_s \Delta h_{f_s}^o R_s + h_{sf} a_{sf} \left(T_p - T_f \right)$$
(23)

The conservation equation of each species, s:

$$\varphi \frac{\partial}{\partial t} (\rho Y_s) + \nabla \cdot (\rho \mathbf{u} Y_s) = -\nabla \cdot (\varphi \mathbf{J}_s) + \varphi R_s$$
(24)

and for He,
$$Y_m = 1 - \sum_{s=1}^{m-1} Y_s$$

The equation of state for an ideal gas:

$$\rho = \frac{P}{\overline{R}T} \left(\sum_{s=1}^{m} Y_s / W_s \right)^{-1} \tag{25}$$

The equation for heat structure:

$$\left[(1 - \varphi)(\rho C)_p \right] \frac{\partial T_p}{\partial t} = \nabla \cdot \left(\lambda_{eff} \nabla T_p \right) + q^{"} - h_{sf} a_{sf} \left(T_p - T_f \right)$$
(26)

All the conservation equations, Eqs. (21)-(24), are discretized as follows:

$$\varphi_i \frac{\rho_i^{n+1} - \rho_i^n}{\Delta t} + \nabla_i \cdot \left(\dot{\rho}^n \mathbf{u}^{n+1}\right) = \varphi_i \sum_i R_{si}^{n+1} , \qquad (27)$$

$$\frac{1}{\varphi_{j}} \frac{\mathbf{u}_{j}^{n+1} - \mathbf{u}_{j}^{n}}{\Delta t} + \frac{1}{\varphi_{j}^{2}} \mathbf{u}_{j}^{n} \cdot \nabla_{j} \left(\mathbf{u}^{n}\right) = -\frac{1}{\overline{\rho}_{j}^{n}} \nabla_{j} \left(P^{n+1}\right) + \frac{1}{\overline{\rho}_{j}^{n} \varphi_{j}} \nabla_{j} \cdot \left[\mu^{n} \nabla \left(\mathbf{u}^{n}\right)\right] - \frac{\overline{\mu}_{j}^{n}}{K_{j}} \mathbf{u}_{j}^{n+1} - \frac{C_{F_{j}} \overline{\rho}_{j}^{n}}{\sqrt{K_{j}}} \left|\mathbf{u}_{j}^{n+1}\right| \mathbf{u}_{j}^{n+1} + \mathbf{g}_{j}^{n} \tag{28}$$

$$\varphi_{i} \frac{\left(\rho H\right)_{i}^{n+1} - \left(\rho H\right)_{i}^{n}}{\Delta t} + \nabla_{i} \cdot \left(\dot{\rho}^{n} \dot{H}^{n} \mathbf{u}^{n+1}\right) = \nabla_{i} \cdot \left[\left(\varphi \lambda_{f} + \lambda_{disp}\right)^{n} \nabla \left(T_{f}^{n}\right)\right] - \nabla_{i} \cdot \left[\sum_{s=1}^{m} \left(\varphi \overline{H}_{s}^{n} \mathbf{J}_{s}^{n}\right)\right] - \varphi_{i} \sum_{s} \Delta h_{f_{s}}^{o} R_{si}^{n+1} + h_{sf_{i}}^{n} a_{sf} \left(T_{p} - T_{f}\right)_{i}^{n}$$

$$(29)$$

$$\varphi_{i} \frac{\left(\rho Y_{s}\right)_{i}^{n+1} - \left(\rho Y_{s}\right)_{i}^{n}}{\Lambda t} + \nabla_{i} \cdot \left(\dot{\rho}^{n} \dot{Y}_{s}^{n} \mathbf{u}^{n+1}\right) = -\nabla_{i} \cdot \left(\varphi \mathbf{J}_{s}^{n}\right) + \varphi_{i} R_{s}^{n+1}$$

$$(30)$$

where a bar (-) indicates average property and a dot (\cdot) indicates donor property which depends on flow direction. In the staggered mesh, i is the index of a scalar cell and j is the index of a momentum cell.

The heat conduction equation, Eq. (26), is solved by the Crank-Nicolson method and coupled with the thermo-fluid calculation explicitly or implicitly.

$$\left[(1 - \varphi) (\rho_{p} C_{p})_{i}^{n} \right] \frac{(T_{p})_{i}^{n+1} - (T_{p})_{i}^{n}}{\Delta t} = q_{N_{i}}^{m} - h_{sf_{i}}^{n} (T_{p_{i}}^{n} - T_{i}^{n}) + \frac{\theta}{Vol_{i}} \nabla_{i} \cdot (\overline{\lambda}_{ef} \nabla T_{p}^{n+1}) + \frac{1 - \theta}{Vol_{i}} \nabla_{i} \cdot (\overline{\lambda}_{ef} \nabla T_{p}^{n})$$

$$a_{e} T_{p}^{c} + a_{w} T_{p}^{w} + a_{e} T_{p}^{e} + a_{b} T_{p}^{b} + a_{t} T_{p}^{t} + a_{s} T_{p}^{s} + a_{p} T_{p}^{n} = b_{c} \quad (32)$$

4.2 Physical models of GAMMA

In order to have a capability to deal with the thermo-fluid transients including an air ingress accident in HTGRs GAMMA consists of physical models developed under the following requirements: Multi-dimensional heat conduction, Multi-dimensional fluid flow, Chemical reactions, Multicomponent molecular diffusion, and Radiation heat transfer.

We developed the extensive graphite oxidation models as shown in Fig 2: kinetics model, mass diffusion model, geometrical, moisture, and moisture effects.

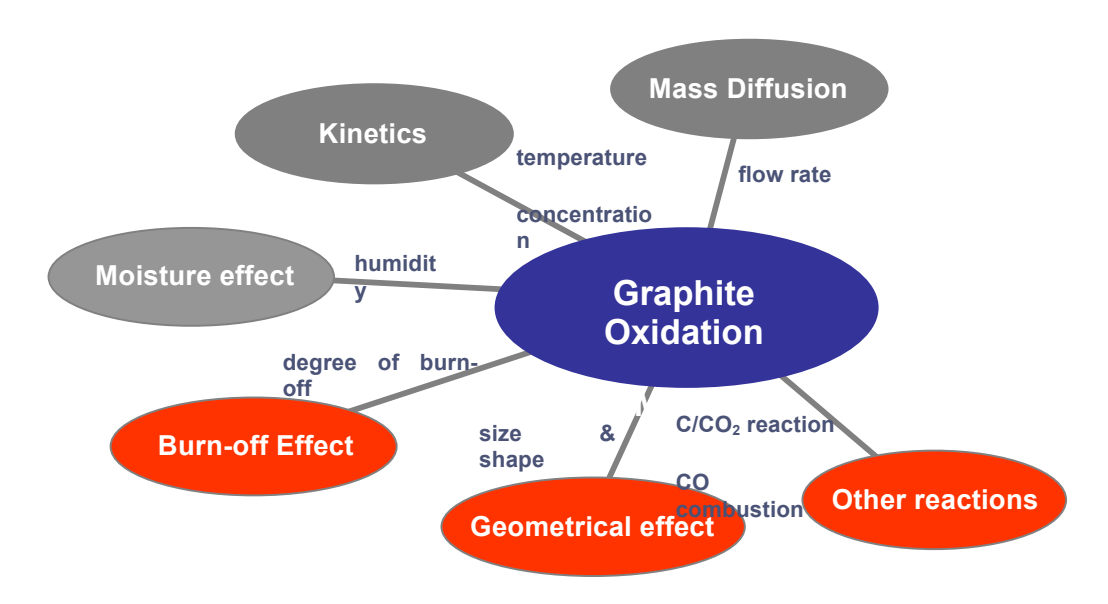


Figure 2. Development of models for rate of graphite oxidation

GAMMA has a gas turbine model to deal with 2-dimensional flow in gas-turbines [23]. We developed a method to predict the characteristics of HTGR helium turbines based on axisymmetric throughflow analysis generally used in the design and analysis of flows in turbines and compressors.

4.3 Assessment

We performed 14 experimental data sets and 1 MIT particle model to validate GAMMA physical models and physical phenomena. Table 2 lists all the test cases collected for the verification and validation of the GAMMA code to ensure the GAMMA capability to predict the basic physical phenomena expected during the transients in a HTGR.

No.	Test Facility	Phenomena
1	Pipe Network, North West Univ., SA	Flow balancing in a complex pipe network
2	Blowdown, North West Univ., SA	Pressure transient and critical flow
3	Duncan & Toor's experiment	Multicomponent molecular diffusion
4	Inverse U-tube single/multiple	Binary molecular diffusion and natural
4	channel test	convection
5	Ogawa's circular tube test	Chemical reactions in a IG-110
6	Takahashi's annular tube test	Chemical reactions in a IG-110
7	VELUNA pebble bed test	Chemical reactions in a pebble bed
8	Inverse U-tube air ingress	Molecular diffusion, natural convection, and
0	experiment	chemical reactions
	HTTR-simulated air ingress	Molecular diffusion, natural convection, and
9	experiment	chemical reactions
	experiment	Multi-D effect on air ingress process
10	Vertical slot experiment	Local circulation effect on molecular diffusion
11	NACOK natural convection test	Natural convection in a pebble bed
12	SANA-1 afterheat removal test	Pebble temperature distributions: steady power
12	SANA-1 attenteat removal test	tests and power ramp up/down tests
13	HTTR RCCS mockup test	Air convection and radiation in a reactor cavity
14	SNU RCCS test	Air convection and radiation in a reactor cavity

Table 2. Assessment matrix for GAMMA V&V

5. Conclusions

Korea has been developing SPACE and GAMMA codes for safety analysis of PWRs and GAMMA, respectively. SPACE consists of up-to-date physical models of two-phase flow dealing with multi-dimensional two-fluid, three-field flow. It has special process models for choking of discharged or internal flow, limitation of countercurrent flow, off-take, water level tracking, and the abrupt change of the flow area. It has a capability to simulate the systems of nuclear power plant. We performed extensive code assessment for its V&V. Further code validation activities against separate effect tests and integral loop tests are scheduled for the end of 2012.

Here, GAMMA for safety analysis of HTGRs has been improved through air-ingressed LOCA analysis code development, gas turbine analysis tool development, and coupling-between TH and reactor physics development. GAMMA is currently expanding through H2 model development and severe-accident model development.

6. Acknowledgements

The author gratefully acknowledges that this was undertaken for 'Conceptual Design and Experimental Validation of Core Technologies for WHEN (Water-Hydrogen-Electricity-Nuclear reactor) System' and financially supported by the Korean Ministry of Education, Science and Technology. Furthermore, the author sincerely acknowledges Sang Jun Ha (KHNP) for offering information on SPACE.

7. Nomenclature

A: Area

B: body force

 $C_{g,gd}$: virtual mass coefficient of drop

 $C_{g,gl}$: virtual mass coefficient of vapor

d: center to center distance vector

e: specific energy

 F_{gl} : interfacial drag coefficient between liquid and vapor phase

 F_{gd} : interfacial drag coefficient between drop and vapor phase

 F_{wg} : wall drag coefficient for vapor phase

 F_{wl} : wall drag coefficient for liquid phase

 F_{wd} : wall drag coefficient for drop phase

 ι_{P}^{E} : conversion factor of face direction to the outward direction from the present cell

h: enthalpy

n: face normal vector

 Q_{n-1} : heat transfer rate from the liquid-vapor interface to vapor phase

 Q_{ij} : heat transfer rate from the liquid-vapor interface to liquid phase

 Q_{v-d} : heat transfer rate from the drop-vapor interface to vapor phase

 Q_{id} : heat transfer rate from the drop-vapor interface to liquid phase

 Q_{l-n} : heat transfer rate from the liquid to non-condensable gas

 Q_{d-n} : heat transfer rate from the drop to non-condensable gas

 S_E : entrainment rate

 S_D : de-entrainment rate

U: velocity vector

 U_n : face normal velocity

V: volume

 α : void fraction

 ε : porosity

 ψ : transport property

 ρ : density

 Γ_i : net vaporization rate at the liquid-vapor interface

 Γ_{LE} : vaporization rate at the liquid-vapor interface

(15/18)

 $\Gamma_{l,c}$: condensation rate at the liquid-vapor interface

 Γ_d : vaporization rate at the droplet-vapor interface

 $\Gamma_{d,E}$: vaporization rate at the drop-vapor interface

 $\Gamma_{d,C}$: condensation rate at the drop-vapor interface

Subscript;

d: dispersed liquid (drop) phase

E: face indicator

g: gas phase

k: face type, 1: x-directional face, 2: y-face, 3: z-face

l: continuous liquid phase

m: mixture

n : non-condensable phase

N: neighbor cell adjacent to the present cell

P: present cell

v: vapor phase

 ϕ : phase indicator

Superscript;

d: donor cell indicator

E: face indicator

n: advanced time

saturated state

8. References

- [1] Ha Sang Jun et al., "Development of the SPACE code for nuclear power plants," Nuclear Engineering and Technology, Vol. 43, No 1, pp 45-62, February 2011
- [2] RELAP5/MOD3.3 Code Manual, Volume I: Code Structure, System Models and Solution Methods, NUREG/CR-5535/Rev 1, December , 2001.
- [3] TRAC-M/FORTRAN90 (VERSION 3.0) Theory Manual, LA-UR-00-910, July, 2000.
- [4] Analysis of FLECHT SEASET 163-Rod Blocked Bundle Data Using COBRA-TF, NUREG/CR-4166, January. 1986.
- [5] M. Robert, M. Farvacque, M. Parent and B. Faydide, CATHARE2 V2.5: a fully validated CATHARE2 version for various applications, Proceedings of the 10th International Topical Meeting on Nuclear Reactor Thermal Hydraulics (NURETH-10) Seoul, South Korea, October 5–9, 2003.
- [6] MARS code manual, volume 1: code structure, system models, and solution methods, KAERI/TR-2812/2004, July 2006.
- [7] "SPACE code manual: Models and Correlations", KAERI, March 8, 2010.
- [8] Churchill, S. W., "Friction-Factor Equation Spans All Fluid-Flow Regimes," Chemical Engineering, pp.91~92, 1977.
- [9] Claxton, K. T., Collier, J. G. and Ward, J. A., "H.T.F.S. Correlation for Two-Phase Pressure Drop and Void Fraction in Tubes," HTFS Proprietary Report HTFS-DR-28, AERE-R7162, 1972.
- [10] Chisholm, D., "A Theoretical Basis for the Lockhart-Martinelli Correlation for Two-Phase Flow," Int. J. Heat and Mass Transfer, vol.10, pp.1767-1778, 1967.
- [11] Okawa, T. and Kataoka, I., "Correlations for the mass transfer rate of droplets in vertical upward annular flow", Int. J. Heat Mass Transfer, 48, pp. 4766-4778, 2005
- [12] Pan, L. and Hanratty, T. J., "Correlation of entrainment for annular flow in horizontal pipes," Int. J. Multiphase Flow, vol.28, pp.385~408., 2002.
- [13] S. V. Paras and A. J. Karabelas, "Droplet entrainment and deposition in horizontal annular flow", Int. J. Multiphase Flow, 17, pp. 455-468, 1991
- [14] J. A. Trapp and V.H. Ransom, A Choked-Flow Calculation Criterion for Nonhomogeneous, Nonequilibrium, Two-Phase Flows, Int. J. Multiphase Flow, Vol. 8, No. 6, pp. 669-681, 1982.
- [15] F. J. Moody, Maximum Flow Rate of a Single Component, Two-Phase Mixture, Trans. of the ASME, J. of Heat Transfer, pp. 134-142, February 1965.

- [16] R. E. Henry and H. K. Fauske, The Two-Phase Critical Flow of One-Component Mixtures in Nozzles, Orifices, and Short Tubes, Trans. of the ASME, J. of Heat Transfer, pp. 179-187, May 1971.
- [17] A. R. Edwards and T. P. O'Brien, Studies of Phenomena Connected with the Depressurization of Water Reactors, Journal of the British Nuclear Energy Society, 9, pp. 125-135, 1970.
- [18] G. B. Wallis, Flooding Velocities for Air and Water in Vertical Tubes, UKAEA, AEEW-R-123, 1961.
- [19] S. G. Bankoff and S. C. Lee, A Brief Review of Countercurrent Flooding Models Applicable to PWR Geometries, Nuclear Safety, Vol. 26, No. 2, pp. 139-152, March-April 1985.
- [20] Hong Sik Lim and Hee Cheon NO, "GAMMA multidimensional multicomponent mixture analysis to predict air ingress phenomena in an HTGR," *Nucl. Sci. Eng.* **152**, 1. (2006)
- [21] Hong Sik Lim and Hee Cheon NO, "Transient multicomponent mixture analysis based on an ICE numerical technique for the simulation of an air ingress accident in a HTGR," J. KNS 36, 375 (2004)
- [22] Hee Cheon NO, et al., "Multi-component Diffusion Analysis and Assessment of GAMMA code and Improved RELAP5 Code," *Nucl. Eng. & Des.*, **237** (2007)
- [23] Hee Cheon NO, Ji Hwan Kim and Hyeun Min Kim, "A Review of Helium Gas Turbine Technology for High-Temperature Gas-Cooled Reactors", *Nuclear Eng. and Tech.*, **Vol. 39**, No 1, 2007